Journal of Materials Chemistry C

Accepted Manuscript

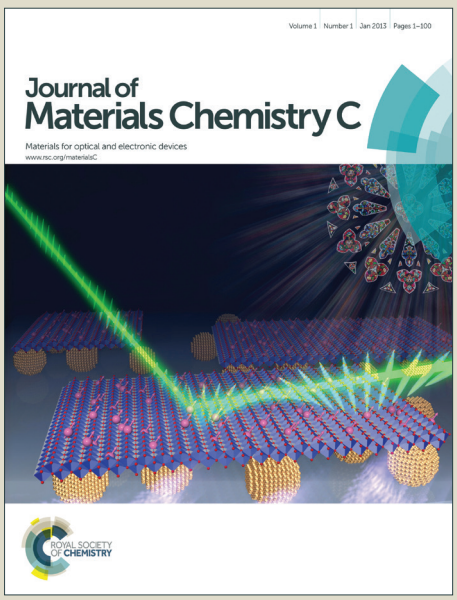

ROYAL SOCIETY OF CHEMISTRY

www.rsc.org/materialsC

Enhanced Field Emission of *p*-type 3*C*-SiC Nanowires with B Dopants and Sharp Corners

Yang Yang[1,2], *Hao Yang*[2], *Guodong Wei*[2], *Lin Wang*[2], *Minghui Shang*[2], *Zuobao Yang*[2], *Bin Tang*[1,*] *and Weiyou Yang*[2,*]

[1] Research Institute of Surface Engineering, Taiyuan University of Technology, Taiyuan City 030024, P.R. China.

[2] Institute of Materials, Ningbo University of Technology, Ningbo City 315016, P.R. China.

Graphical Table of Contents

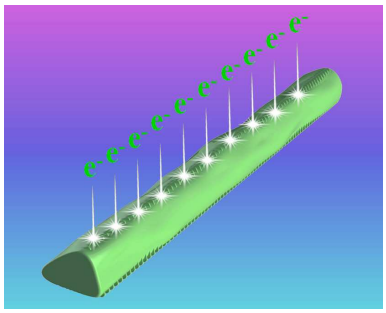

We report the enhanced field emission of B-doped SiC nanowires with a low turn on field and enhanced high-temperature stability.

[*] Corresponding authors. E-mails: tangbin@tyut.edu.cn (B. Tang) and weiyouyang@tsinghua.org.cn (W. Yang)
Tel: +86-574-87080966, Fax: +86-574-87081221.

ABSTRAC

The field emission with a low turn-on field and well stability is critically important and highly desired for the practical application of nanostructures in electron emitters. In present work, we reported the growth of *p*-type 3*C*-SiC nanowires with B dopants and sharp corners via catalyst-assisted pyrolysis of polymeric precursor. The morphologies, structures and field emission (FE) properties of the resultant SiC nanowires were investigated. FE measurements suggest that the B-doped SiC nanowires have excellent FE performances with a low turn-on field of 1.35Vμm^{-1} and high field enhancement factor of ~4895. More importantly, the current emission fluctuation of B-doped nanowires with an applied field of 1.88 Vμm^{-1} at 200 °C could be improved to ~11% from ~22% of the undoped counterparts, suggesting that the high-temperature FE stability of SiC nanowires could be significantly enhanced by the B dopants. The excellent FE performances could be attributed to the special *p*-type triangular prism-like nanostructures with B dopants and numerous sharp corners on the prism edges, which could reduce the effective work function and remarkably increase the emission site density.

1. Introduction

Silicon carbide (SiC) one-dimensional (1D) nanostructures have attracted extensive attention due to their promising applications in nanodevices with respect to their superior mechanical properties, high thermal conductivity, low thermal-expansion coefficient, good thermal-shock resistance, as well as their chemical stability and electron affinity.[1-3] Among these unique properties, the field emission (FE) properties of diverse SiC 1D nanostructures (*e.g.,* nanowires,[4-9] nanorods,[10] nanoneedles,[11] nanobelts,[12] nanotubes,[13] bamboo-like nanowires,[14-16] and hexagonal nanoprisms[14,17]) were investigated widely in the past decades, owning to their prospective applications in flat panel displays and other electronic nanodevices.

According to the Fowler-Nordheim (F-N) theory,[18] there are mainly two routes to enhance the FE performance: one is to enhance the field enhancement factor (β), and the other is to reduce the work function (Φ). For instance, it was reported that the FE of SiC emitters can be significantly enhanced through decreasing the radii of curvature of the nanostructures (*i.e.,* make them with sharp tips) to enhance the β values,[11,19-21] and via increasing the aspect ratios and aligning the growth of the nanostructure.[22-24] Zhang *et al.* reported that Al dopants within SiC nanowires could favor a more localized state near the Fermi energy level,[25] thus leading to the reduce of work function and enhancement of electron emission. Recently, Chen *et al.* reported that SiC quasialigned nanoarrays with N dopants exhibited outstanding FE properties with low turn-on fields of 1.90-2.65 $V\mu m^{-1}$ and threshold fields of 2.53-3.51 $V\mu m^{-1}$, respectively.[26] In addition, the increase of the emission sites is another effective route to enhance the FE for a given nanostructures.[27] These suggested that the FE properties could be remarkably enhanced once the SiC nanostructures could be tailored with suitable doping, sharp

tips and more emission sites.[25] However, most of previous works were carried out just under room temperature. To the best of our knowledge, there is scarce work focused on the high-temperature field emission stabilities of SiC nanostructures, which is critically important for the exploration of SiC nanodevices with respect to the current induced Joule heat.

As for the bulk SiC, many works reported that the B dopants could bring them a higher solubility and faster diffusion coefficient. This impurity is of interest, because B dopants incorporated in SiC can not only form acceptor levels but also make the smooth P-N junctions and diodes with S-type I-V characteristic.[28] As compared to Si-C covalent, more stable B-C atom pair can be formed during the doping process within the SiC induced by the B dopants,[29] which could make the SiC-based devices more qualified to work in harsh environments such as high temperatures. That is to say, it is promising that B-doped SiC low-dimensional nanostructures might possess more excellent FE properties with enhanced high-temperature stability. However, except for its bulk counterparts,[30-32] there are few works focused on the B-doped SiC nanostructures.

Here, we report the growth of the *p*-type 3*C*-SiC nanowires via catalyst assisted pyrolysis of polymeric precursors. We focus on two points in this work as following: one is to design the structures with numerous sharp corners on a single nanowire to profoundly increase the electron emission sites based on the local field enhancement effect, thus leading to lower the turn-on fields; The other is to realize the B doping of SiC nanostructures, which is expected to enhance the high-temperature field emission stability. The experimental results suggest that the as-synthesized *p*-type 3*C*-SiC nanowires with B dopants and sharp corners exhibit an excellent FE properties with a very low turn-on field and

enhanced high-temperature emission stability, suggesting that they could be a promising candidate to be used as electronic display nanodevices under high-temperature harsh work conditions (*e.g.,* the electron guns of field emission scanning electron microscopy).

2. Experimental procedure

The B-doped 3*C*-SiC nanowires were synthesized by catalyst-assisted pyrolysis of polymeric precursor of polyborosilazanes (PBSZ) (Institute of Chemistry, Chinese Academic of Science, China). The raw materials of PBSZ, with a composition of $Si_{0.64}BC_{0.78}N_{1.53}O_{0.25}$, were commercial available and used directly without further treatment. In a typical procedure for the growth of B-doped SiC nanowires, ~0.5 g of liquid PBSZ was placed on the bottom of a high-purity graphic crucible (purity: 99%) with a graphic paper to be utilized as the substrate located on the top of the crucible. The substrate of graphite paper was firstly treated for catalyst introduction by being immersed in ethanol solution of 0.05 mol/L $Co(NO_3)_2$ (purity: 99%) and dried in air at room temperature (RT) naturally. Then the crucible configuration was put into a graphite-heater vacuum furnace and pyrolysis at 1550 ºC under Ar atmosphere (99.9% purity, 0.1MPa). The pyrolysis process was carried out by heating up to the desired temperature of 1550 ºC from RT with a heating rate of 25 °C/min, and directly decreasing the temperature from 1550 to 1100 ºC with a cooling rate of 15 °C/min, followed by furnace to ambient temperature. For comparison, pure SiC nanowires (without B dopants) were also synthesized with the raw materials of polysilazane (Institute of Chemistry, Chinese Academic of Science, China) and otherwise similar experimental conditions.

The obtained products were characterized with using field emission scanning electron microscopy

(FESEM, S-4800, Hitachi, Japan), high-resolution transmission electron microscopy (HRTEM, JEM-2100F, JEOL, Japan) equipped with energy dispersive X-ray spectroscopy (EDS, Quantax-STEM, Bruker, Germany), and X-ray diffraction (XRD, D8 Advance, Bruker, Germany) with a Cu-*Ka* radiation (λ = 1.5406 Å). The measurements of FE properties of SiC nanowires were performed on a home-built high vacuum field emission setup with a base pressure of ~3.0×10^{-7} Pa at RT and 200 ºC, respectively. The current-voltage (*I-V*) and the current-time (*I-t*) curves were recorded on a Keithley 248 unit with a detection resolution of 0.1 fA. The distance between the cathode (*i.e.,* the surface of SiC nanowire grown on the graphite substrate) and the anode was fixed at ~800 μm.

3. Results and discussion

SEM was first employed to characterize the morphology and structure of the as-synthesized samples. Fig. 1(a-b) display the SEM images of the as-synthesized samples grown randomly on the graphite substrate under different magnifications. The length and diameter of the nanowires are typically sized in ~10 microns and ~500 nanometers, respectively (Fig. 1(b)). Based on the observations under SEM, the number of nanowires is *ca.* ~130000/cm^2 (Fig. 1(a)), showing the relatively low density of the wires grown on the graphite substrate. Closer observations in different view angles (Fig. 1(c-e)) reveal that the nanowires possess a unique triangular prism-like body and slowly convergent root. Unlike the conventional nanowires often with a smooth surface, it is interesting that all of the nanowires possess a very rough one. It seems that there are numerous sharp corners decorated on the edges of the triangular prism-like nanowires. This special structure can enhance the FE properties due to the fact that these sharp corners can act as the efficient electron emitting sites caused by the local field enhancement effect.[33,34] In the previous work, we reported the growth of *p*-type SiC nanowires with a very smooth

surface dominated by the vapor-liquid-solid (VLS) mechanism with a triangular prism shape under pyrolysis at 1450 °C with an enough long annealing time of 1 h, which was attributed to the minimization of the surface energy induced by high-temperature annealing.[35] As compared to current synthesis procedure (*i.e.*, heating up to 1550 ºC followed by cool down from 1550 to 1100 ºC without any annealing time and with a cooling rate of 15°C/min), it suggests that the formation of the triangular prism-like nanowires with numerous sharp corners on the edges could be attributed to the uncompleted process of surface energy minimization of the laterally faceted crystal planes via atomic diffusion. That is to say, in our case, the growth of the triangular prism-like SiC wires with sharp corners on the edges could be accomplished by tailoring the pyrolysis experimental conditions. Fig. 1(f) and (g) display the as-synthesized undoped SiC nanostructures under different magnifications. As compared to the B-doped sample, the grown SiC nanowires have a higher density (*ca.* ~230000/cm^2) (Fig. 1(f)) with a relatively smooth surface.

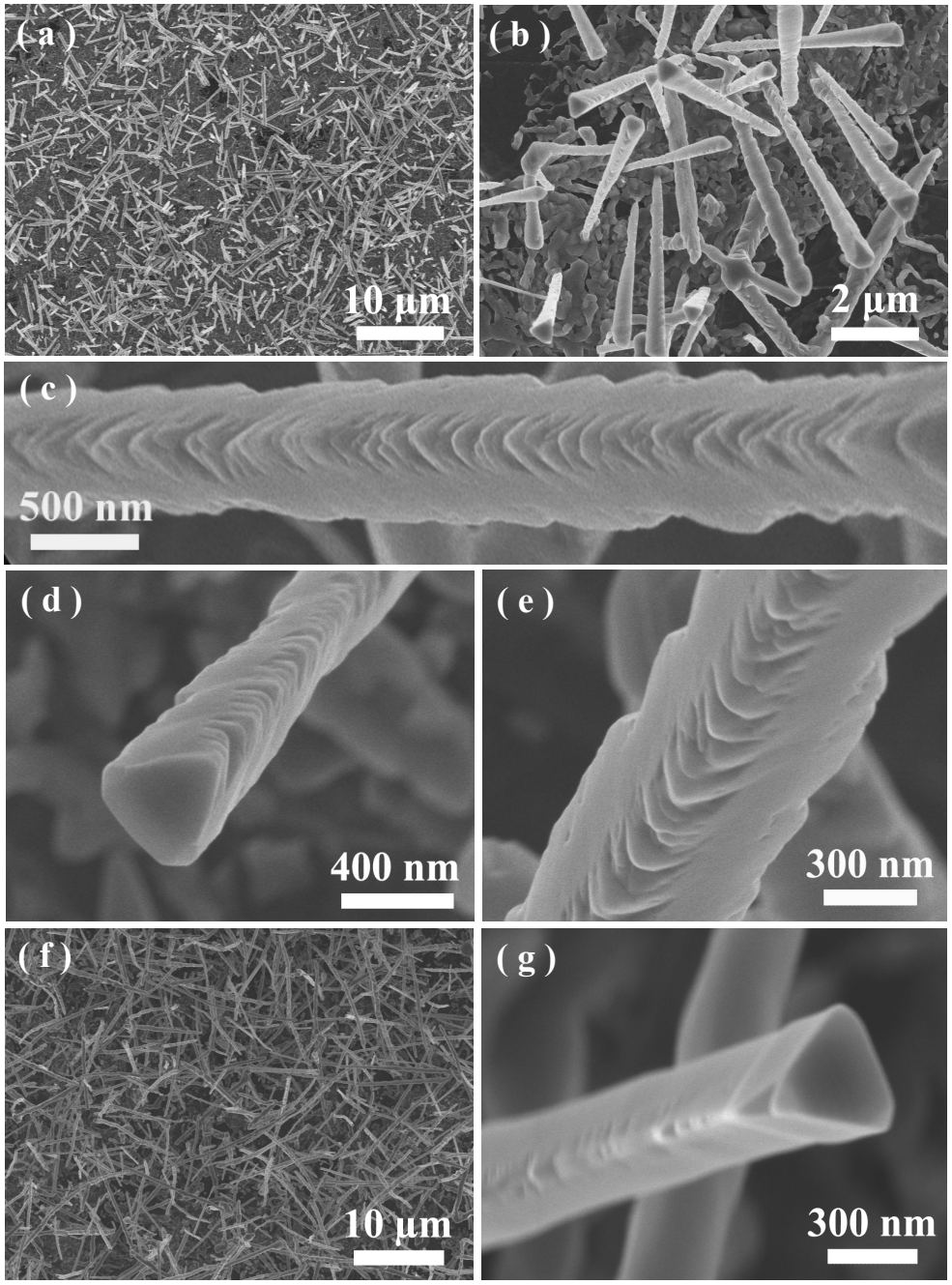

Fig. 1 (a-b) Typical SEM images of the grown B-doped nanowires under low magnifications. (c-e) Closer observations of a single B-doped nanowire showing numerous sharp corners grown on the triangular prism-like wire body in different view angles. (f-g) typical SEM images of the undoped nanowires under different magnifications.

Characterizations of the obtained B-doped SiC nanowires were further performed by TEM. Fig. 2(a)

displays a typical TEM image of the nanowires under a low magnification. It further confirms that the nanowire has a rough surface. Fig. 2(b) presents a typical SAED pattern of the wire recorded from the marked area of A in Fig. 2(a), which is identical over the entire nanowire, indicating that the nanowire is single crystalline and can be indexed to 3*C*-SiC (JCPDS Card No. 29-1129). Fig. 2(c) is the corresponding HRTEM image, in which the inter-planar spacing of two neighboring lattice fringes is *ca.* ~0.25 nm, fitting to the plane distance of cubic SiC (111). Both SAED pattern and HRTEM image suggest that the nanowires grow along the [111] direction. Fig. 2(d) shows the representative mapping of B element within the wire body obtained from EDS under TEM, suggesting its uniform spatial distribution with an average concentration of ~5.03 *at.*%. The typical XRD patterns recorded from B-doped sample+substrate and pure substrate are presented in Fig. 2(e), which correspond to the red and black curves, respectively. It suggests that all of the peak sets can be indexed well to the only phase of 3*C*-SiC (JCPDS Card No.29-1129), except for the diffractions from the graphite substrates (JCPDS Card No. 26-1076). The low intensity peak at about 2θ=34° is ascribed to the stacking faults. The sharp diffraction peaks indicate that the resultant wires possess a good crystallinity. Fig. 2(f) shows the enlarged pattern of (111) diffraction peak. Compared with the standard data (JCPDS Card No. 29-1129) marked as the blue dashed line, the (111) peak of the obtained nanowires makes a shift to a higher angle. The shift of 0.084º in 2θ can be attributed to the distortion in the crystalline lattice structure caused by substitution of smaller B atoms (radius: 0.095nm) to the Si atoms (radius: 0.134nm),[36] suggesting that the incorporation of B dopants into SiC lattice should be dominated mainly by substitutional solid solutions.[37,38]

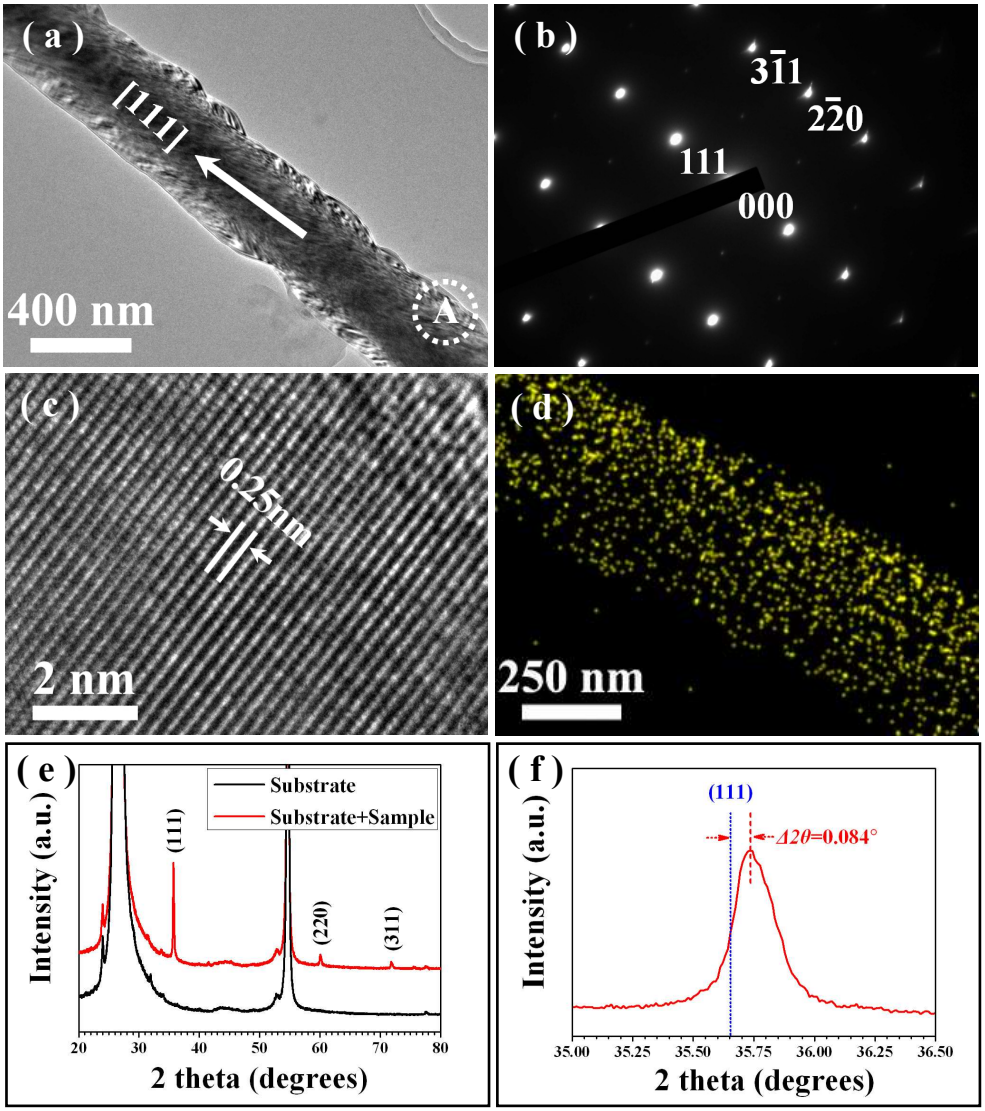

Fig. 2 (a) A typical TEM image of a single B-doped SiC wire. (b-c) Corresponding SAED pattern and HRTEM image of the B-doped SiC wire recorded from the area of A in (a). (d) Element mapping of B dopants within the wires. (e) XRD patterns of B-doped wires+substrate (red line) and substrate (black line). (f) An enlarged XRD pattern showing the red shift of diffraction peak for (111) plane of B-doped wires. The dashed blue dot line responses to the standard data (JCPDS Card No. 29-1129).

The FE property measurements of the resultant SiC nanowires were carried out in a vacuum chamber with the cathode-anode distance fixed at ~800 μm. The *J-E* curve shown in Fig. 3(a) illustrates the field emission current density (*J*) as a function of the applied electric field (*E*) for the B-doped SiC

emitters at RT. The emitters exhibit the excellent FE performances with a turn-on field (defined as the electric field to obtain a current density of 10 μA/cm^2) and the threshold field (defined as the electric field to obtain a current density of 10 mA/cm^2) of 1.35 and 1.70 Vμm^{-1}, respectively, which are much smaller than those of the most reported SiC nanostructure-based field emitters,[9,15,16,39-45] regardless of the low density of the grown wires on the substrate (Fig. 1(a)). The relatively low maximum emission current might be mainly attributed to the low densities of the grown SiC nanowires (Fig. 1(a), ~130000/cm^2) and the low applied maximum electric fields (< 3 V μm^{-1}) in our experiments (Fig. 3(a)). It is known that the field emission current is mainly due to the tunneling of electrons through the surface barrier, which is described by simplified *F-N* equation:[18]

$$J = (A\beta^2 E^2 / \Phi)\exp[-B\Phi^{3/2}(\beta E)^{-1}]$$

where J is emission current density, E is the applied electric field, Φ is the work function, β is the field enhancement factor, and A and B are constants, corresponding to 1.54×10^{-6}AeVV^{-2} and 6.83×10^3 (eV)$^{-3/2}$μm^{-1}, respectively. The corresponding *F-N* curve, which reveals the relationship between $ln(J/E^2)$ and $1/E$, is shown in Fig. 3 (b). The plot shows an approximately linear relationship, implying that the electron emission from the B-doped SiC emitter at RT follows the traditional *F-N* emission mechanism. From the slope of the F-N curve, the β of the B-doped SiC emitter is *ca.* ~4895 by using the work function of undoped SiC (4.0 eV) under RT,[46] which is quite larger than those in the previous work.[5,9,20,25,26,47] These results suggest that the FE performances of as-synthesized SiC nanowires have been significantly enhanced with a very low turn-on field and high field enhancement factor, which could be mainly attributed to the following two points: i) The B dopants. B dopants incorporated into the SiC via the formation of substitutional solid solutions (schematically shown in Fig. 3(c)) might favor a more localized state near the Fermi energy level,[25] which pins the Fermi level moving forward to the

vacuum conduction band. This could make the reduce of work function[48,49] and favor a more facile electron transfer from the Fermi level to the vacuum conduction band, leading to the remarkable enhancement of the FE properties of the SiC nanowires; ii) The sharp corners. In current case, numerous sharp corners have been grown around the edges of triangular prism-like SiC nanowires. Owning to the local field enhancement effect, the sharp corners could act as efficient electron emitting sites,[33,34] which implies that the unique saw-like edges of the triangular prism-like SiC nanowires have profoundly increased the density of the emitting sites (schematically shown in Fig. 3(d)), thus leading to the significant enhancement of the FE properties with a low turn-on field.

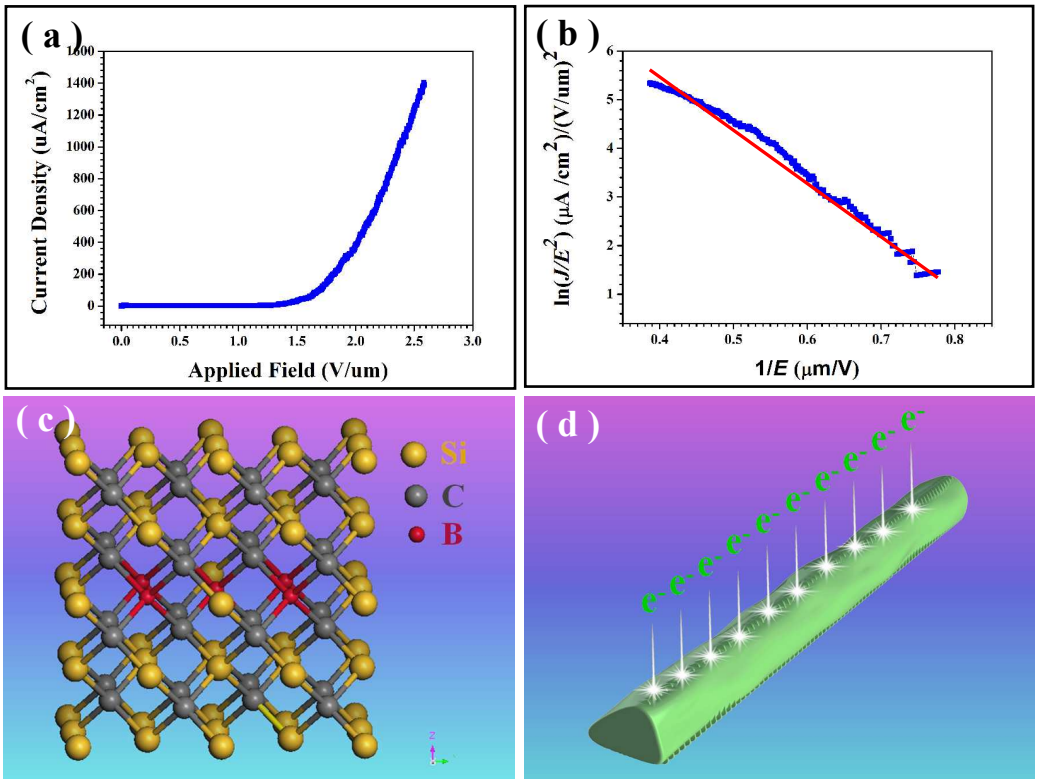

Fig. 3 (a-b) A typical *J*–*E* curve at RT and corresponding F–N plot of the B-doped SiC wires, respectively. (c) Crystal structure of SiC with substitutional solid solutions of B dopants. (d) Schematic illustration for the electron emission from the B-doped wires with numerous sharp corners on the edge.

Then we come to the point how about the field emission stability of the obtained SiC nanowires. In

general, the stability of temperature-dependent field emission could be decreased with the increase of environmental temperatures, due to the contribution from the thermionic electron emission and the decrease in the effective work function.[20] Fig. 4(a) and (b) show the stabilities of the field emission current at the applied field of 1.88 $V\mu m^{-1}$ over 10 h for B-doped triangular prisim-like SiC nanowires and pure counterparts at RT (~27 °C) and high temperature of 200 °C, respectively. Both of FE currents are stable without obvious degradation during the monitoring time of 10 h. It seems that the current fluctuations are *ca.* ~14% and 11% corresponding to the emitters worked at RT and 200 °C, respectively, disclosing that the enhanced stability of the B-doped SiC nanowires worked under high temperature as compared to that worked under RT. For comparison, the electron emission stabilities of the undoped sample (Fig. 1(f) and (g)) were also characterized with otherwise similar experimental conditions (*i.e.,* with applied field: 1.88 V/μm, monitoring time: 10 h), as shown in Fig. 4 (c) and (d). The current fluctuations of the undoped sample worked under RT and 200 °C are *ca.* ~ 9% and ~22%, respectively. As compared for the undoped sample itself, the electron emission stability for working at 200 °C exhibits much worse than that working at RT, which is decreased by more than one time (~22% *vs* ~9%). Meanwhile, as compared between the B-doped and undoped emitters, the stability of the B-doped sample worked under 200 °C exhibit much better than that of undoped sample, which is enhanced by more than one time (~11% *vs* ~22%). These results strongly confirm that the high-temperature field emission stability of the SiC nanostructures could be significantly enhanced by B dopants. The detailed mechanism for this enhancement is not clear currently and needs to be further investigated. However, the enhanced high-temperature filed emission stability of the SiC nanowires should be attributed to the B dopants, which could generate more stable B-C atom pairs as compared to Si-C species in interstitial sites, leading to a higher solubility and better heat dispersion of SiC.

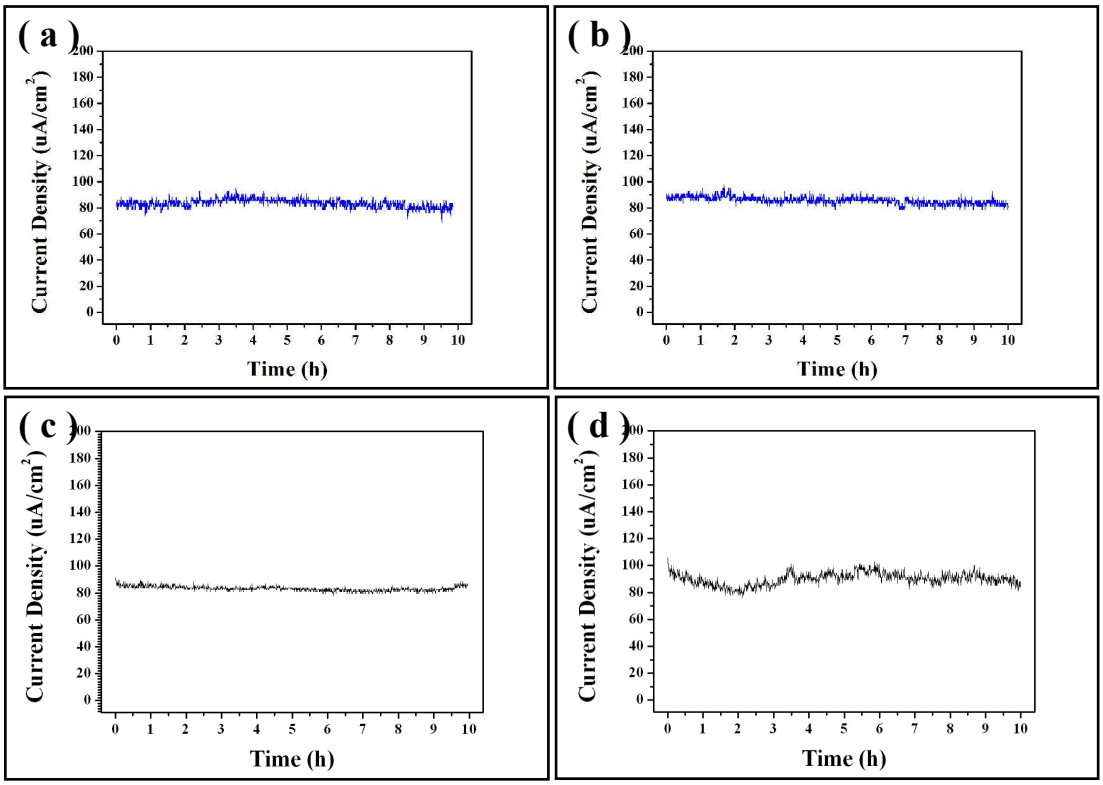

Fig. 4 (a-b) FE emission stabilities of B-doped SiC wires under RT and 200 ºC, respectively. (c-d) FE emission stabilities of undoped SiC wires under RT and 200 ºC, respectively.

4. Conclusions

In summary, we demonstrate the growth of *p*-type 3*C*-SiC nanowires via pyrolysis of polyborosilazane with $Co(NO_3)_2$ as the catalysts, which possess numerous sharp corners on the prism edges and a uniform spatial distribution of B dopants. FE measurements suggest that the B-doped SiC nanowires have excellent FE performances with a low turn-on field of 1.35Vμm^{-1} and high field enhancement factor of ~4895. Meanwhile, the current emission fluctuation of B-doped nanowires with an applied field of 1.88 Vμm^{-1} at 200 °C could be improved to ~11% from ~22% of undoped SiC nanowires, suggesting that the high-temperature FE stability of SiC nanowires could be significantly enhanced by the B dopants. The excellent FE performances could be attributed to the special *p*-type

triangular prism-like nanostructure with B dopants and numerous sharp corners on the prism edges, which could reduce the effective work function and remarkably increase the emission site density. Current work suggests that incorporation of B dopants into SiC nanowire could be an effective strategy to enhance their high-temperature FE emission stability, which could push forward the exploration of electronic nanodevices to be worked under high temperatures.

Acknowledgements

The work was financially supported by 973 program (Grant No. 2012CB326407), National Natural Science Foundation of China (NSFC, Grant Nos. 51372123 and 51202115), and Key Technology Program of Ningbo Municipal Government (Grant No. 2013B6007).

References

1. J. B. Casady and R. W. Johnson, *Solid-State Electron.*, 1996, **39**, 1409.
2. E. W. Wong, P. E. Sheehan and C. M. Lieber, *Science*, 1997, **277**, 1971.
3. J. Fan, X. Wu and P. K. Chu, *Prog. Mater Sci.*, 2006, **51**, 983.
4. Z. Li, M. Zhang and A. Meng, *CrystEngComm*, 2011, **13**, 4097.
5. R. Wu, K. Zhou, J. Wei, Y. Huang, F. Su, J. Chen and L. Wang, *J. Phys. Chem. C*, 2012, **116**, 12940.
6. Z. Pan, H. L. Lai, F. C. Au, X. Duan, W. Zhou, W. Shi, N. Wang, C. S. Lee, N. B. Wong and S. T. Lee, *Adv. Mater.*, 2000, **12**, 1186.
7. G. Yang, H. Cui, Y. Sun, L. Gong, J. Chen, D. Jiang and C. Wang, *J. Phys. Chem. C*, 2009, **113**, 15969.
8. R. Wu, K. Zhou, X. Qian, J. Wei, Y. Tao, C. H. Sow, L. Wang and Y. Huang, *Mater. Lett.*, 2013, **91**, 220.
9. M. G. Kang, H. J. Lezec and F. Sharifi, *Nanotechnology*, 2013, **24**, 065201.

10. Y. Sun, H. Cui, G. Z. Yang, H. Huang, D. Jiang and C. X. Wang, *CrystEngComm*, 2010, **12**, 1134.
11. Z. S. Wu, S. Z. Deng, N. S. Xu, J. Chen, J. Zhou and J. Chen, *Appl. Phys. Lett.*, 2002, **80**, 3829.
12. G. Zou, C. Dong, K. Xiong, H. Li, C. Jiang and Y. Qian, *Appl. Phys. Lett.*, 2006, **88**, 071913.
13. H. Cui, J. Zhou, G. Z. Yang, Y. Sun and C. X. Wang, *CrystEngComm*, 2011, **13**, 902.
14. R. Wu, B. Li, M. Gao, J. Chen, Q. Zhu and Y. Pan, *Nanotechnology*, 2008, **19**, 335602.
15. G. Shen, Y. Bando and D. Golberg, *Cryst. Growth Des.*, 2007, **7**, 35.
16. G. Shen, Y. Bando, C. Ye, B. Liu and D. Golberg, *Nanotechnology*, 2006, **17**, 3468.
17. T. Y. Zhang, M. Luo and W. K. Chan, *J. Appl. Phys.*, 2008, **103**, 104308.
18. R. H. Fowler and L. Nordheim, *Proc. R. Soc. London, Ser. A*, 1928, **119**, 173.
19. X. Fang, L. Wu and L. Hu, *Adv. Mater.*, 2011, **23**, 585.
20. G. Wei, H. Liu, C. Shi, F. Gao, J. Zheng, G. Wei and W. Yang, *J. Phys. Chem. C*, 2011, **115**, 13063.
21. Y. Tang, H. Cong, Z. Chen and H. Cheng, *Appl. Phys. Lett.*, 2005, **86**, 233104.
22. X. Fang, Y. Bando, G. Shen, C. Ye, U. Gautam, P. Costa, C. Zhi, C. Tang and D. Golberg, *Adv. Mater.*, 2007, **19**, 2593.
23. M. Jha, R. Patra, S. Ghosh and A. K. Ganguli, *J. Mater. Chem.*, 2012, **22**, 6356.
24. X. Fang, J. Yan, L. Hu, H. Liu and P. S. Lee, *Adv. Funct. Mater.*, 2012, **22**, 1613.
25. X. Zhang, Y. Chen, Z. Xie and W. Yang, *J. Phys. Chem. C*, 2010, **114**, 8251.
26. S. Chen, P. Ying, L. Wang, G. Wei, J. Zheng, F. Gao, S. Su and W. Yang, *J. Mater. Chem. C*, 2013, **1**, 4779.
27. J. H. He, R. Yang, Y. L. Chueh, L. J. Chou, L. J. Chen and Z. L. Wang, *Adv. Mater.*, 2006, **18**, 650.
28. A. Andreev, M. Anikin, A. Lebedev, N. Poletaev, A. Strelchuk, A. Syrkin and V. Chelnokov, *Institute of Physics Conference Series, Bristol*, 1994, **137**, 271.
29. R. Rurali, E. Hernández, P. Godignon, J. Rebollo and P. Ordejón, *Phys. Rev. B*, 2004, **69**, 125203.
30. R. Klein and L. Leder, *Phys. Rev.*, 1961, **124**, 1046.
31. L. Liao, W. F. Zhang, H. B. Lu, J. C. Li, D. F. Wang, C. Liu and D. J. Fu, *Nanotechnology*, 2007, **18**, 225703.
32. Q. Y. Zhang, J. Q. Xu, Y. M. Zhao, X. H. Ji and S. P. Lau, *Adv. Funct. Mater.*, 2009, **19**, 742.
33. Y. Saito, K. Hata and T. Murata, *Jpn. J. Appl. Phys.*, 2000, **39**, L271.

34. R. R. Devarapalli, R. V. Kashid, A. B. Deshmukh, P. Sharma, M. R. Das, M. A. More and M. V. Shelke, *J. Mater. Chem. C*, 2013, **1**, 5040.
35. F. Gao, W. Feng, G. Wei, J. Zheng, M. Wang and W. Yang, *CrystEngComm*, 2012, **14**, 488.
36. S. Agathopoulos, *Ceram. Int.*, 2012, **38**, 3309.
37. Z. He, L. Wang, F. Gao, G. Wei, J. Zheng, X. Cheng, B. Tang and W. Yang, *CrystEngComm*, 2013, **15**, 2354.
38. F. Gao, W. Yang, H. Wang, Y. Fan, Z. Xie and L. An, *Cryst. Growth Des.*, 2008, **8**, 1461.
39. A. Meng, M. Zhang, J. Zhang and Z. Li, *CrystEngComm*, 2012, **14**, 6755.
40. H. Cui, L. Gong, G. Yang, Y. Sun, J. Chen and C. Wang, *Phys. Chem. Chem. Phys.*, 2011, **13**, 985.
41. J. Chen, Q. Shi and W. Tang, *Mater. Chem. Phys.*, 2011, **126**, 655.
42. H. Cui, Y. Sun, G. Yang, J. Chen, D. Jiang and C. Wang, *Chem. Commun.*, 2009, 6243.
43. Y. Yang, G. Meng, X. Liu, L. Zhang, Z. Hu, C. He and Y. Hu, *J. Phys. Chem. C*, 2008, **112**, 20126.
44. Y. Ryu, Y. Tak and K. Yong, *Nanotechnology*, 2005, **16**, S370.
45. K. W. Wong, X. T. Zhou, F. C. K. Au, H. L. Lai, C. S. Lee and S. T. Lee, *Appl. Phys. Lett.*, 1999, **75**, 2918.
46. X. Fang, Y. Bando, U. K. Gautam, C. Ye and D. Golberg, *J. Mater. Chem.*, 2008, **18**, 509.
47. D. W. Kim, Y. J. Choi, K. J. Choi, J. G. Park, J. H. Park, S. M. Pimenov, V. D. Frolov, N. P. Abanshin, B. I. Gorfinkel and N. M. Rossukanyi, *Nanotechnology*, 2008, **19**, 225706.
48. J. C. Charlier, M. Terrones, M. Baxendale, V. Meunier, T. Zacharia, N. Rupesinghe, W. Hsu, N. Grobert, H. Terrones and G. Amaratunga, *Nano Lett.*, 2002, **2**, 1191.
49. C. C. Chen, C. C. Yeh, C. H. Chen, M. Y. Yu, H. L. Liu, J. J. Wu, K. H. Chen, L. C. Chen, J. Y. Peng and Y. F. Chen, *J. Am. Chem. Soc.*, 2001, **123**, 2791.